Simulation of ultrasonic inspection of composite using bulk waves: Application to curved components

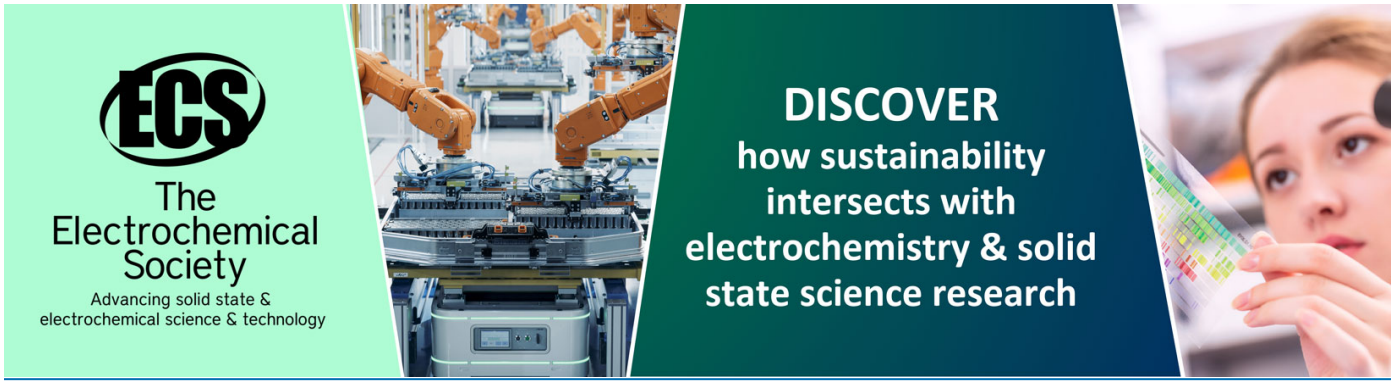

Journal of Physics: Conference Series **269** (2011) 012022 doi:10.1088/1742-6596/269/1/012022

Simulation of ultrasonic inspection of composite using bulk waves: application to curved components

S Journiac[1], N Leymarie[1], N Dominguez[2] and C Potel[3]
[1]CEA, LIST, Département Imagerie et Simulation pour le Contrôle, F-91191 Gif-sur-Yvette, France.
[2]EADS France Innovation Works, ZAC de Saint Martin du Touch, 18 rue de Marius Terce, 31300 Toulouse, France.
[3]Université du Maine, Avenue Olivier Messiaen, 72085 Le Mans, France.

E-mail: sophie.journiac@cea.fr

Abstract. The increasing use of composite materials in aircraft, particularly carbon-fiber reinforced samples, presents new challenges for Non-Destructive Testing (NDT) operations to ensure reliable inspections. The aircraft industry is showing a growing interest in the simulation of NDT techniques applied to such materials, which exhibit strong anisotropy. Simulation tools are needed to predict beam deviations that may arise for curved or tilted parts in complex specimen. A main issue is the modelling of the wave propagation and flaw scattering inside a homogeneous medium considering a continuously variable anisotropic orientation. Previous works have presented a way to model these media. This method consists in decomposing them into a set of homogeneous sub-sections with constant orientations. This approximation allows us to use straight paths over homogeneous sections but the main drawback is that it introduces artificial boundaries leading to numerical instabilities. The new model deals with a continuously variable anisotropy. It is based on a ray calculation for an inhomogeneous medium using an iterative time-step method. This method consists in solving for each time step a system of differential equations taking into account the continuous anisotropic orientation variation along the trajectory.

1. Introduction

Composites are increasingly being used by the aerospace industry as a substitute for metals. About a quarter of the structure of the Airbus A380 is made up of lightweight carbon-fiber-reinforced plastic (CFRP). The geometry of structures being optimized, they become more and more complex, presenting sometimes tightly curved shapes. Especially concerning stiffeners, the radius dimension can be very small. Simulation tools are of great interest to optimize NDT techniques of such structures.

The CFRP structures are made of several unidirectional layers of carbon fibers embedded in epoxy matrix. These structures exhibit a strong anisotropy between the axis and the plane of the stack. Previous works concerning beam calculation in CFRP were already implemented in CIVA [1], [2], [3]. The approach is based on the search of equivalent energy direction through the stacking sequence of the layered structure. The equivalent mechanical properties of the effective medium are deduced from the equivalent energy direction. In the case of complex geometries, the only way to model beam

propagation is to divide the component into a set of homogeneous sub-sections with a local disorientation following the geometry [3]. In the case of curved composites, this approximation can be used but leads to some numerical artefacts due to the presence of fictive interfaces. In this paper, we proposed to extend the ray-based model developed in CIVA [4] to calculate the beam propagation in curved composites without any sample discretization. The idea is to consider a local anisotropic orientation that follows continuously the curvature of the fibers.

First, we present the mathematical formulation used to determine local mechanical properties in CFRP curved composites. Then, the ray based theory adapted to smoothly inhomogeneous anisotropic material is introduced to predict beam field amplitude. Finally, validations and comparisons of beam calculations are performed for cylindrical samples with different radii of curvature.

2. Formulation of mechanical properties in a layered CFRP composite with a curved shape

Based on observations of layered curved composites, we considered that each ply follows the global curvature of the sample. Following this assumption, we proposed a general formulation of the mechanical anisotropic properties of a layered CFRP composite in a Cartesian coordinate system. The spatial dependency of the mechanical properties is deduced for curved shaped composites.

Let us denote by C^{ref} the elastic stiffness tensor for a reference flat layered composite structure. In a Cartesian canonical basis $(\vec{e}_1, \vec{e}_2, \vec{e}_3)$, its formulation is:

$$C^{ref} = \sum_{ijkl} c_{ijkl}^{ref} \vec{e}_i \otimes \vec{e}_j \otimes \vec{e}_k \otimes \vec{e}_l \tag{1}$$

where c_{ijkl}^{ref} represent the components of the 4-th order tensor C^{ref} of a reference plate. Considering that the curved sample is obtained as the distortion of a plate into a curved surface, we define the transformation Φ from the flat to the curved structure (cf. Figure 1).

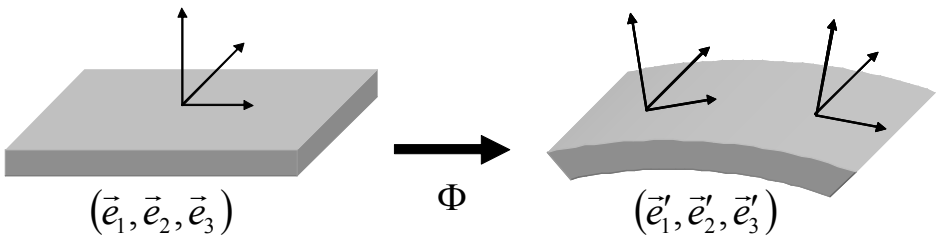

Figure 1. Illustration of the Φ transformation of a flat plate into a curved shell surface

We assume that the basis composed by the normal and tangents of the median surface remains orthonormal after transformation. Applied to a curved composite ply, the physical meaning of this transformation is that the local anisotropy axis is following the fiber curvature.

Considering that the stiffness tensor for the curved plate is conserved in the local orthonormal basis $(\vec{e}'_1, \vec{e}'_2, \vec{e}'_3)$ after transformation, and then we have:

$$C = \sum_{ijkl} c_{ijkl}^{ref} \vec{e}'_i \otimes \vec{e}'_j \otimes \vec{e}'_k \otimes \vec{e}'_l \,, \tag{2}$$

where the vectors $\vec{e}'_j$ of the local basis verify the relation $\vec{e}'_j \cdot \vec{e}_i = \Phi_{i,j} = J_{ij}$, matrix J being the Jacobian matrix for transformation Φ. Note that this matrix is normalized in order to neglect any dilatation effect due to the curvature. The elastic properties are also invariant with respect to the normal of the median plane before and after transformation. The matrix J is then equivalent to a local transformation matrix.

Combining relations (1) and (2), we obtain a relationship between the elastic constants of the curved sample c_{ijkl} and the elastic constants of the reference plate c_{ijkl}^{ref}:

$$c_{ijkl} = \sum_{mnrs} c_{mnrs}^{ref} J_{im} J_{jn} J_{kr} J_{ls} \tag{3}$$

Finally, we obtain a spatially-dependent relationship of variables c_{ijkl} as a function of the reference elastic constants (spatially invariant) and the Jacobian matrix deduced from the spatial transformation Φ. So the mechanical properties evaluated for a curved shape correspond to a smoothly inhomogeneous anisotropic material since Φ is a regular function.

3. Pencil model in smoothly inhomogeneous anisotropic material

The pencil model is a ray-based model developed for homogeneous anisotropic material [4]. In this case, ray trajectories are straight lines. A pencil is a collection of rays emanating from the point source and diverging slightly. One can define the axial ray, along the geometrical path, and the paraxial rays, belonging to the envelope of the pencil. We proposed here to extend this model to smoothly inhomogeneous anisotropic media.

3.1. Ray trajectory evaluation

3.1.1. *Theoretical equation governing ray propagation.* Main theoretical results are presented in depth by V. Cerveny in his book "Seismic Ray Theory" [5] and [6]. V. Cerveny established a general model that describes ray propagation in smoothly inhomogeneous anisotropic media. These ray equations have been developed for seismic applications but they are still valid for ultrasound since wave path is long in comparison with wavelength.

Using the Eikonal equation and the Christoffel equation, a differential expression of the ray position $\vec{x}$ and its associated wave slowness $\vec{S}$ with the travel time of the ray T is obtained:

$$\begin{cases} \dfrac{dx_i}{dT} = c_{ijkl} S_l P_j P_k = V_{e_i} \\ \dfrac{dS_i}{dT} = -\dfrac{1}{2} \dfrac{\partial\left(\rho^{-1} c_{jkln}\right)}{\partial x_i} S_k S_n P_j P_l \end{cases}, \tag{4}$$

where P_i are the components of the normalized polarization associated to the ray mode and ρ is the densitv. Let us notice in the first equation that the expression of the energy velocity vector denoted $\vec{V}_e$ can be identified.

Note that in the homogeneous case the variations of the elastic constants being of zero, the slowness variation with respect to travel time is null too. Therefore the slowness of the ray is a constant and the trajectory is a straight line following the energy direction as shown in Figure 2.

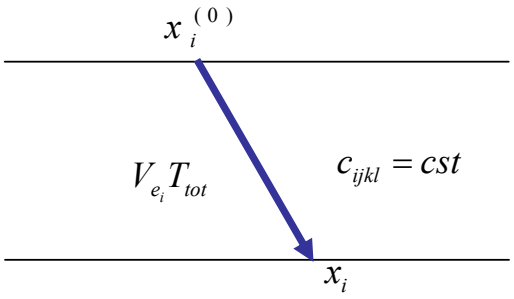

$$\frac{dS_i}{dT} = 0 \Rightarrow S_i = S_i^{(0)}$$
$$\frac{dx_i}{dT} = V_{e_i} \Rightarrow x_i = x_i^{(0)} + V_{e_i} \times T_{tot}$$

Figure 2. Trajectory obtained in homogeneous case.

In the general inhomogeneous case, the two equations of the differential system (4) are interdependent. Variations of the position depend on the associated slowness and the variations of the slowness depend on the gradient of stiffnesses with the position. Except for some particular cases, the only way to determine the ray trajectory consists in using an iterative scheme to solve the initial value problem:

$$\frac{dY}{dT} = F(Y). \tag{5}$$

where the variable Y represents the parameters of the ray as a function of travel time such as $Y = (x_i, S_i)$.

3.1.2. *Numerical evaluation of ray trajectory by an iterative scheme.* To solve the differential system (5) with a numerical resolution, a fourth-order Runge-Kutta (RK4) scheme is used [7]. Using this numerical scheme, the error made is of the fourth order with respect to the travel time step ΔT.

The wave mode is specified by initial conditions imposed to the ray tracing system. For an initial source point and an initial phase direction $\vec{n}$, the norm of the slowness vector $\vec{S}$ must be one of the three roots of the Christoffel equation:

$$\left| S^2 \rho^{-1} c_{ijkl} n_j n_k - \delta_{il} \right| = 0. \tag{6}$$

Then, for each step of the calculation, we evaluate simultaneously perturbations of the position of the ray and its slowness. During the iterative process, the slowness vector does not satisfy exactly the Christoffel equation (6). In order to stabilize the iterative scheme, the norm of the slowness is corrected if the determinant of equation (6) is over a certain value. This way, we construct an iterative time-step propagation as represented in Figure 3:

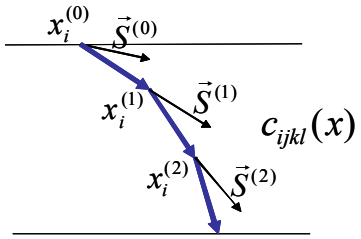

Figure 3. Principle of the iterative time-step propagation.

3.2. Extension of the pencil method

For field calculation, after determining ray trajectories, we need to calculate the associated amplitude. To determine the amplitude for each ray we have extended the principle of the pencil method. The pencil method [4] is based on the energy conservation in a ray tube, which is still valid in our case this condition being satisfied by the transport equation [6].

To evaluate the pencil propagation matrix in a smoothly inhomogeneous medium, we consider that the medium is homogeneous between each step of trajectory calculations. This way, we neglect the distortion due to local inhomogeneity between paraxial rays and the axial ray.

So if we introduce the pencil propagation matrix L_n which describes the parameter evolution of the ray tube during its propagation at step *n,* the global propagation matrix is simply the product of

matrices L_n for each calculation step. Then after N iterations, the pencil vector Ψ_N at the calculation point and the pencil vector at the source Ψ_0 are linked by the formula:

$$\Psi_N = (L_0 L_1 ... L_N)\Psi_0 . \tag{7}$$

4. Numerical results and discussion

To validate our continuously variable model, numerical results are compared. We consider this model and a description of the sample as a set of homogeneous sub-sections with a local orientation of anisotropy. In previous work, S. Deydier has shown that the piecewise description remains valid for complex shapes described in the Cartesian basis [3]. But it appears that this generates some numerical artifacts due to fictive interfaces, which can be critical for cases with a strong local elastic gradient.

4.1. Application to a cylindrical geometry: the stiffener case

Let us consider the case of a sample with cylindrical geometry, for instance a stiffener. In this case, the fibers follow the component with a constant curvature.

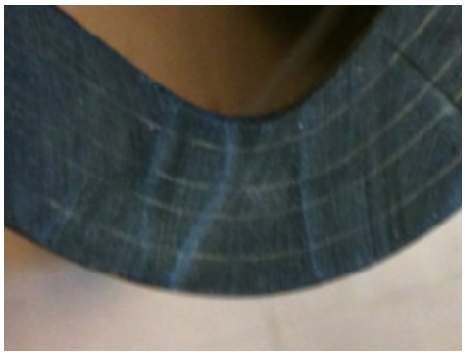

Figure 4. Picture of the curved part of a stiffener

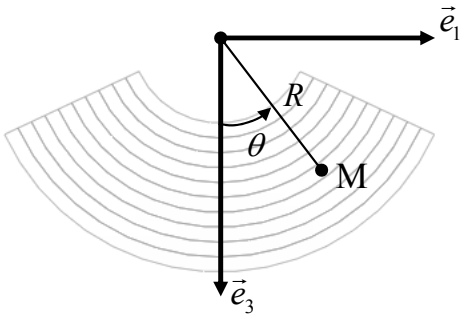

Figure 5. Modelling of the sample in Figure 4 by a curved panel with a constant radius

In the case of a stiffener with cylindrical geometry, the transformation Φ is analytically known. For every point M in the cylindrical sample, the Jacobian matrix J can be defined as a function of angle θ used in Figure 5:

$$J(M) = \begin{pmatrix} \cos\theta & 0 & -\sin\theta \\ 0 & 1 & 0 \\ \sin\theta & 0 & \cos\theta \end{pmatrix}. \tag{8}$$

Combining this expression of the Jacobian with the general equation (3), we obtain an analytical formulation of the stiffness tensor in a cylindrical sample as a function of point M. To solve the ray tracing system (4), we can also deduce the variations of the elastic constants according to the position with the formula invariant with the variable R such as:

$$\frac{\partial c_{ijkl}}{\partial x_i} = \frac{\partial c_{ijkl}}{\partial \theta} \times \frac{\partial \theta}{\partial x_i} . \tag{9}$$

So all elements to solve the system (4) being known, numerical simulations have been performed in the case of a cylindrical shape. In the following part numerical results are presented.

4.1.1. *Rays trajectories.* In our case, trajectories obtained with piecewise descriptions and calculated with the continuous description are considered. Results for several discretizations are considered: 5, 11, 21 and 39 sectors. In Figure 6, some examples of piecewise description are illustrated showing the variable orientations according to the normal of fibers at the centre of each sector.

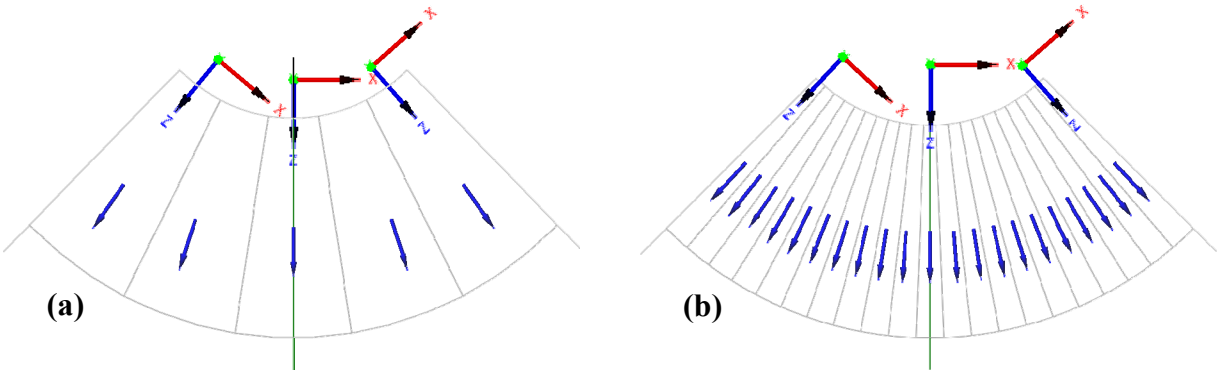

Figure 6. Example of piecewise description with (a) 5 and (b) 21 sectors.

Let us consider a stiffener with an inner radius of curvature of 10 mm and a thickness of 13.2 mm, the stiffness tensor is known locally in Cartesian coordinates in an abbreviated Voigt form, numerical values are detailed in table 1.

Table 1. Stiffness tensor values used to simulate ray propagation in a CFRP curved composite.

	C_{11}^{ref}	C_{12}^{ref}	C_{13}^{ref}	C_{22}^{ref}	C_{23}^{ref}	C_{33}^{ref}	C_{44}^{ref}	C_{55}^{ref}	C_{66}^{ref}
Stiffness (GPa)	96.96	67.46	5.65	119.70	5.92	12.57	4.25	3.58	20.04

The material is considered to be orthotropic and shows a strong anisotropy between the x-y plane and the z direction (cf. table 1).

We have also compared the trajectory of rays radiated from a 6.25 mm diameter plane transducer. For piecewise description, the ray propagation corresponds to straight line in each sector and the refraction of the ray is evaluated at each interface. For the continuous description, we use the iterative scheme previously presented in section 3.

Numerical results obtained in the four cases are illustrated in Figure 7. The finer the piecewise description is, the more the plotted trajectories converge to the continuous description trajectories. We observe that for this tiny radius of curvature the localization of the focal point is very sensitive to the piecewise description. It confirms that this curved sample has to be considered with a high degree of precision in order to obtain an accurate beam width.

The trajectories for the description with 39 sectors and for continuous description being quasi identical (cf. Figure 7 (c) and (d)), this study validates our model for trajectories and we look now at the problem of transmitted fields.

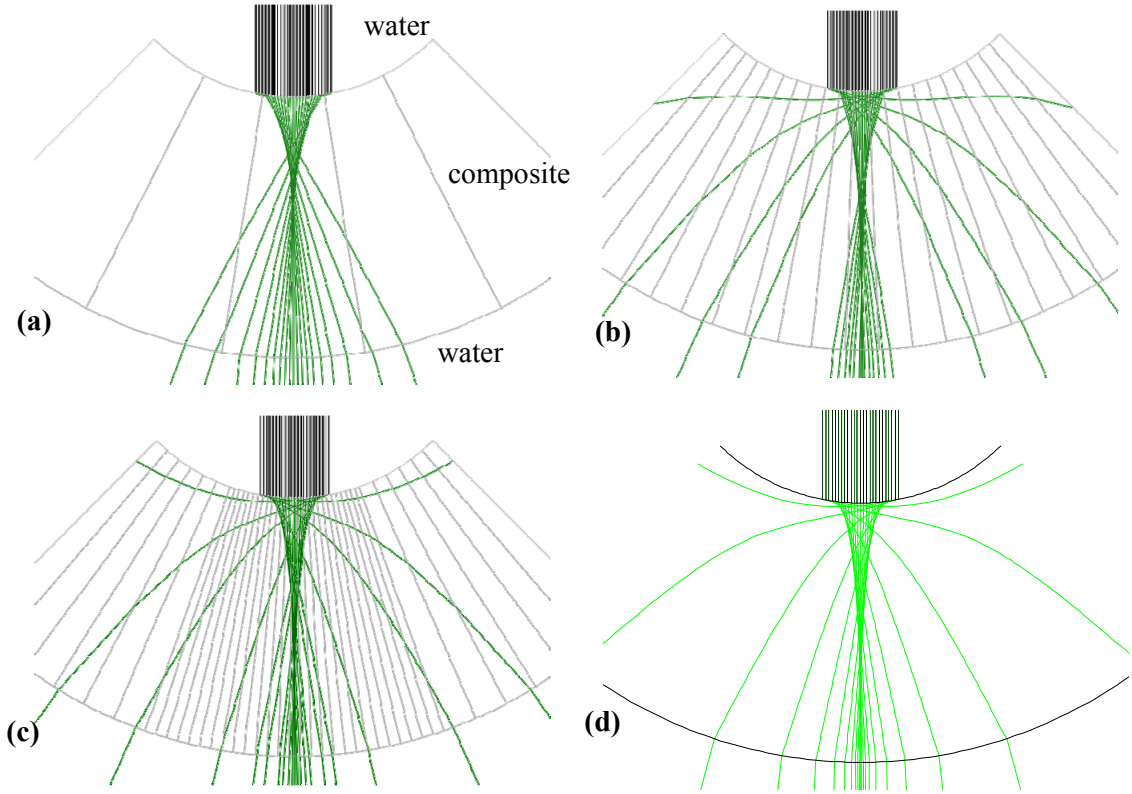

Figure 7. Trajectories obtained for the piecewise description with (a) 5, (b) 21, (c) 39 sectors and (d) with the continuous description.

4.1.2. *Transmitted field.* As before, transmitted fields for continuous and piecewise descriptions are compared. The calculation is done on a line at 25 mm form the cylindrical sample in water (cf. Figure 8) for a 6.25 mm diameter plane transducer with a central frequency around 2.25 MHz.

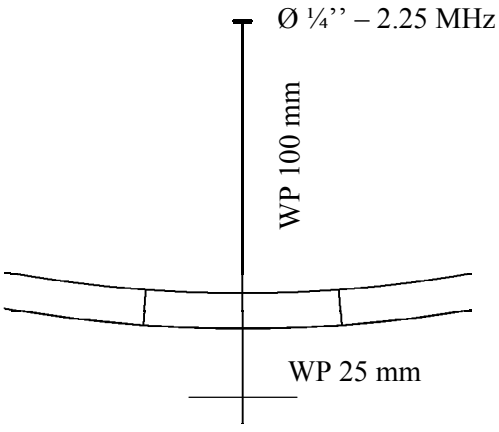

Figure 8. Configuration used for validation of the transmitted field calculation

At first, let us consider the case of a sample with a large radius of curvature. For example we choose a radius of curvature of 500 mm. In this situation, effects of the curvature are small and the piecewise description is known as valid [3]. Let us report results for the piecewise description with 5 sectors:

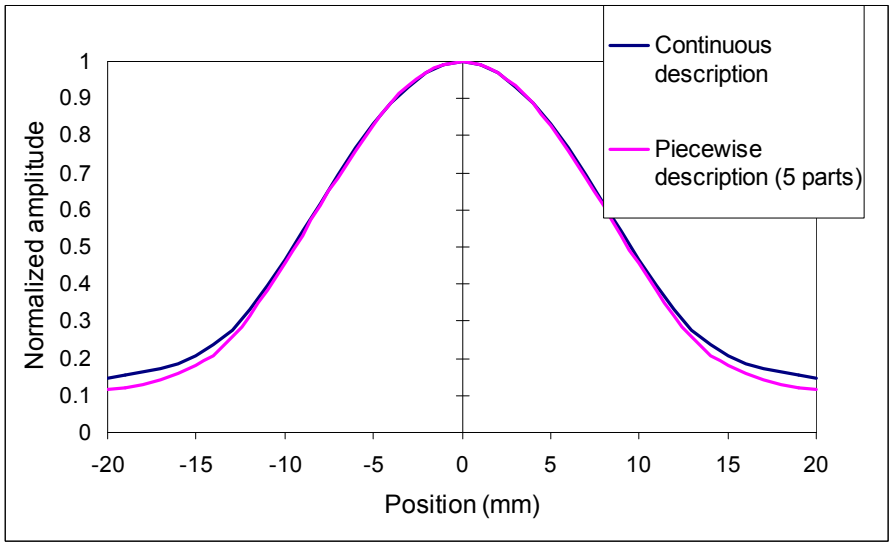

Figure 9. Transmitted field for a radius of curvature of 500mm.

There is a very good agreement between the two curves as we can see in Figure 9. In particular beam widths correspond perfectly. With this example we can validate our new model for the case of a large radius of curvature.

Now, let us look the same problem for a smaller radius, of 10 mm. For this case the continuous description and a description with 39 sectors are compared as already done for trajectories (cf. Figure 7 (c) and (d)).

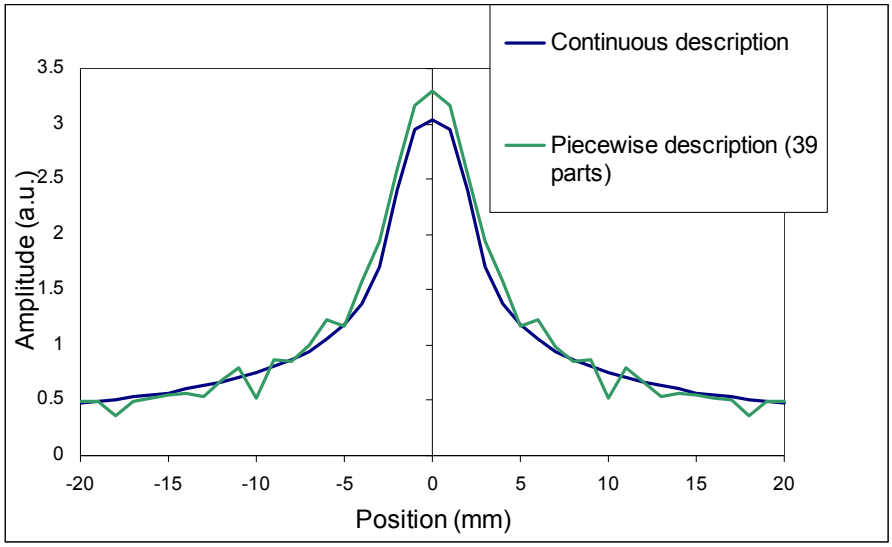

Figure 10. Transmitted field for a radius of curvature of 10mm.

Some numerical artifacts appear due to the interfaces created by the discretization of the piecewise description. These fictive interfaces lead to problems for field calculations; rays arriving exactly on the interfaces are not taken into account and numerical artifacts are created. So in the case of small radii of curvature, we need to have a finer description with many sectors to be confident with the result. But this leads to more numerical artifacts due to artificial interfaces.

The Figure 10 shows us that the transmitted fields obtained with the two descriptions are similar in terms of amplitude and beam width.

5. Conclusion

In this paper, we propose a ray based model for propagation in curved composites. This continuous model was validated for a quasi-plane specimen by comparing with a piecewise model. In the case of small radii of curvature, results presented here are a first promising step before an experimental validation. There are advantages to this continuous description: numerical artefacts due to fictive interfaces are avoided. But in return the iterative numerical scheme is costly in time. So future works will focus in optimizing the numerical scheme, the time step selected can be adapted with local elastic variations inside the component. Experimental comparisons with composite samples provided by EADS are in progress.

References

[1] CIVA software platform for simulating NDT techniques (UT, EC, RT) http://www-civa.cea.fr
[2] Lonné S, Lhémery A, Calmon P, Biwa S and Thévenot F 2004 Modeling of ultrasonic attenuation in unidirectional fiber reinforced composites combining multiple-scattering and viscoelastic losses *Review of Progress in QNDE* **23**, ed D O Thompson and D E Chimenti (Melville: AIP Conf. Proc. **700**) 875
[3] Deydier S, Leymarie N, Calmon P and Mengeling V 2006 Modeling of the ultrasonic propagation into carbon-fiber-reinforced epoxy composites, using a ray theory based homogenization method *Review of Progress in QNDE* **25**, ed D O Thompson and D E Chimenti (Melville: AIP Conf. Proc. **820**) 972
[4] Gengembre N and Lhémery A 2000 Pencil method in elastodynamics: application to ultrasonic field computation *Ultrasonics* **38** 495
[5] Cerveny V 2001 *Seismic Ray Theory* chapter 2 (Cambridge: Cambridge University Press)
[6] Cerveny V 2001 *Seismic Ray Theory* chapter 3 (Cambridge: Cambridge University Press)
[7] Numerical Recipes Third Edition http://www.nrbook.com/nr3/